VLA OBSERVATIONS OF RADIO GALAXIES WITH EXTENDED LOBE EMISSION: 3C 79 AND 3C 430

STEVEN R. SPANGLER, STEVEN T. MYERS, AND JEAN J. POGGE
Department of Physics and Astronomy, The University of Iowa, Iowa City, Iowa 52242
Received 21 March 1984; revised 16 July 1984

ABSTRACT

Dual-frequency (1.446 and 4.885 GHz) total intensity and polarimetric observations have been made with the VLA of the radio galaxies 3C 79 and 3C 430. These sources are characterized by extended lobe and/or radio bridge emission. 3C 430 possesses an asymmetric structure which may indicate large-scale inhomogeneities in a confining medium. This source also displays Faraday rotation fluctuations which are apparently unrelated to depolarization, suggesting an origin in an external medium. Our polarization observations suggest that the magnetic fields in both sources possess large-amplitude, random components. In the case of 3C 79, we observe a correlation between depolarization and position-angle rotation. It is unclear whether this is due to internal Faraday rotation, indicating the presence of a large-scale magnetic field, or a Faraday-rotating screen external to the radio-emitting material.

I. INTRODUCTION

While recent studies of the extended extragalactic radio sources have tended to emphasize the radio jets, other structural features such as the hot spots, extended lobes, and bridges, also are of considerable interest. Within the context of the beam models (Blandford and Rees 1974), the hot spots represent "working surfaces" created by the interaction of the beam with an intergalactic medium, and serve as sites of energetic electron acceleration. The lobes and bridges are then naturally interpreted as due to electrons which "leak out" of the hot spots.

One can easily think of limiting cases describing the processes by which this electron transport occurs. If the allowed particle streaming speed is small (on the order of a hydrodynamic speed), then it is probable that the particles are being left behind as the hot spot advances into an intergalactic medium. Such a situation has been assumed in the analyses of Burch (1977, 1979b) and Winter *et al.* (1980). If, on the other hand, high particle streaming speeds can occur, then processes of transport which emphasize free-particle motion would be more favored. Observations of the sort presented in this paper can help indicate which type of electron transport is occurring.

In addition to providing information about energetic electron transport processes, polarimetric observations of lobes and bridges can provide information on the nature of the magnetic fields in radio sources. In particular, we would like to know if they are of the partially ordered sort proposed by Laing (1981).

The sources described in this paper, 3C 79 and 3C 430, were chosen for investigation because previous observations had revealed extended lobe and/or bridge emission. In this respect, these sources are similar to ones we have previously studied, 3C 166 (Spangler and Bridle 1982) and 3C 411 (Spangler and Pogge 1984). The observations discussed in this paper will illustrate the characteristics which are relevant to the aforementioned questions of electron transport and magnetic field structure, as well as providing observations which are of use to other investigators.

Previous observations of these sources have been presented by Burch (1979a,b). Burch's 2.7-GHz observations provide a useful complement to the observations presented here.

The galaxy associated with 3C 79 is of visual magnitude 18.6 and redshift 0.256; that associated with 3C 430 is of 15th magnitude and redshift 0.055 (Burbidge and Crowne 1979).

II. OBSERVATIONS

Observations were made with the VLA in the "A array" configuration in June 1982 (1.4-GHz observations), the "B array" (1.4- and 5-GHz observations) in August 1982, and the "C array" (5-GHz observations) in April 1983. A summary of details relevant to the observations is given in Table I, which lists the observing time for each source and array, and the phase calibrator used. Characteristics of the resulting maps are also given in Table I. For each source and frequency, we give the total (zero spacing) flux, as well as the noise levels in the Stokes parameter I, Q, and U maps. The latter quantities were measured in regions of the maps far from the source. For all total intensity (Stokes parameter I) maps, the sum of the CLEAN components was equal, within the measurement error, to the single-dish flux. In general, the procedures used in acquisition and analysis of data were similar to those previously described by Spangler and Bridle (1982) and Spangler and Pogge (1984).

The only comment we feel needs to be made in support of Table I regards the fact that we did not succeed in obtaining C array observations of 3C 430 at 4.9 GHz. The purpose of these observations was to ensure that sufficiently short spacings were included in the maps. An (apparently successful) attempt was made to obtain the short spacings "in projection" via observations at low elevations. To determine the effect of the missing short spacings, we compared spectral-index maps made with the 4.9-GHz maps and 1.4-GHz maps computed (a) with all data and (b) with only the (u, v) coverage obtained in the 4.9-GHz observations. No systematic differences were noted between the two spectral-index maps. Specifically, measurements along the source axis showed that spectral indices from the two maps agreed to within 0.01 in the presence of a total change of 0.20. Furthermore, in the CLEAN phase of map analysis, we were able to recover all of the single-dish flux. In summary, we believe that the 4.9-GHz maps of 3C 430 are not missing low-surface brightness features, and that the slight spectral index gradients discussed below are real.

Map analysis followed the standard procedure of mapping, cleaning, and two iterations of phase self-calibration

 0004-6256/84/101478-09$00.90

TABLE I. Summary of observations of 3C 79 and 3C 430.

	Observing Time (Hours)			
	Array			
	A	B	C	Total
3C 79 (1.446 GHz)	1.5	0.4		1.9
3C 79 (4.885 GHz)		1.0	1.9	2.9
3C 430 (1.446 GHz)	2.0	0.5		2.5
3C 430 (4.885 GHz)		1.2	--	1.2
Phase Calibrators				
3C 79: 0319 + 121				
3C 430: 2146 + 608				
Map Characteristics				
	S_{TOT} (Jy)	rms Fluctuation (mJy/beam) I	Q	U
3C 79 (1.446 GHz)	4.30	0.24	0.14	0.13
3C 79 (4.885 GHz)	1.31	0.13	0.05	0.05
3C 430 (1.446 GHz)	7.30	0.27	0.16	0.15
3C 430 (4.885 GHz)	3.32	0.18	0.08	0.08

using the NRAO AIPS (Astronomical Image Processing System) software package. The resolution of the maps is 1".5 (FWHM) in the case of 3C 79 and 1".8 for 3C 430.

III. OBSERVATIONAL RESULTS

Figure 1 displays our 1.4-GHz maps of the sources, contoured to emphasize the low-surface brightness emission. As will be the case for the remainder of the images presented below, the maps have been rotated, by $-10°$ in position angle for 3C 79, and by 55° in the case of 3C 430.

The positions and flux densities of the central components are given in Table II. Our observations indicate flat spectra for both central components in the frequency range 1.4–5 GHz.

Figures 2 and 3 present our maps of 3C 79 and 3C 430. The format is the same in both figures. For panels (a) and (b), the left and right subpanels contain the 1.4- and 4.9-GHz images, respectively. Panel (a) contains contour plots of total intensity, contoured at the same levels at the two frequencies to facilitate comparison. Panel (b) presents the polarization position angles [$\chi \equiv 1/2 \tan^{-1}(U/Q)$]. The lengths of the vectors are proportional to the fractional linear polarization, and a single contour of the total intensity furnishes a boundary to the image. Pixels were blanked at points where the total intensity fell to less than five times the rms noise level, or where the polarized intensity fell to less than ten times the noise level in the Q and U maps. Panel (c) displays the position angle *difference* map ($\chi_{1.4} - \chi_5$), and panel (d) presents a coarse-resolution representation of the distribution of 1.4–5 GHz spectral index.

We now discuss the salient observational features of these sources, as revealed in Figs. 2 and 3. To avoid confusion in reference to our rotated maps, the following convention will be adhered to. The right-hand lobe of 3C 79 (as seen in our figures) will be referred to as N_p (for North-preceding), since this describes its orientation on the sky. The left-hand lobe is then denoted by S_f. Similarly, the right-hand lobe of 3C 430 will be denoted as S_p, and the left N_f.

a) 3C 79

Perhaps the most striking observational feature of 3C 79 is the noncollinearity of structure in the N_p lobe. The prominent hot spot lies well above the main part of the lobe emission. Furthermore, the high-brightness region directly behind the hot spot bends away from the lobe. An intrusion in the lower part of the N_p lobe [marked "A" in Fig. 2, panel (a)] may indicate the interaction of the lobe with external material possessing pressure comparable to that of the radio-emitting material. Inspection of Fig. 2(d) shows that the spectrum of this lobe is noticeably steeper than that of the hot spot, indicating more pronounced or advanced synchrotron-radiation losses.

The S_f lobe is more nearly collinear, with a secondary hot spot [labeled "B" in Fig. 2, panel (a)], and an interior, local maximum in the radiation intensity. The spectral index map Fig. 2(d) shows a gradual increase of spectral index with increasing distance from the hot spot.

The polarization data [Figs. 2(b)] reveal further pronounced differences between the two lobes. The N_p lobe pos-

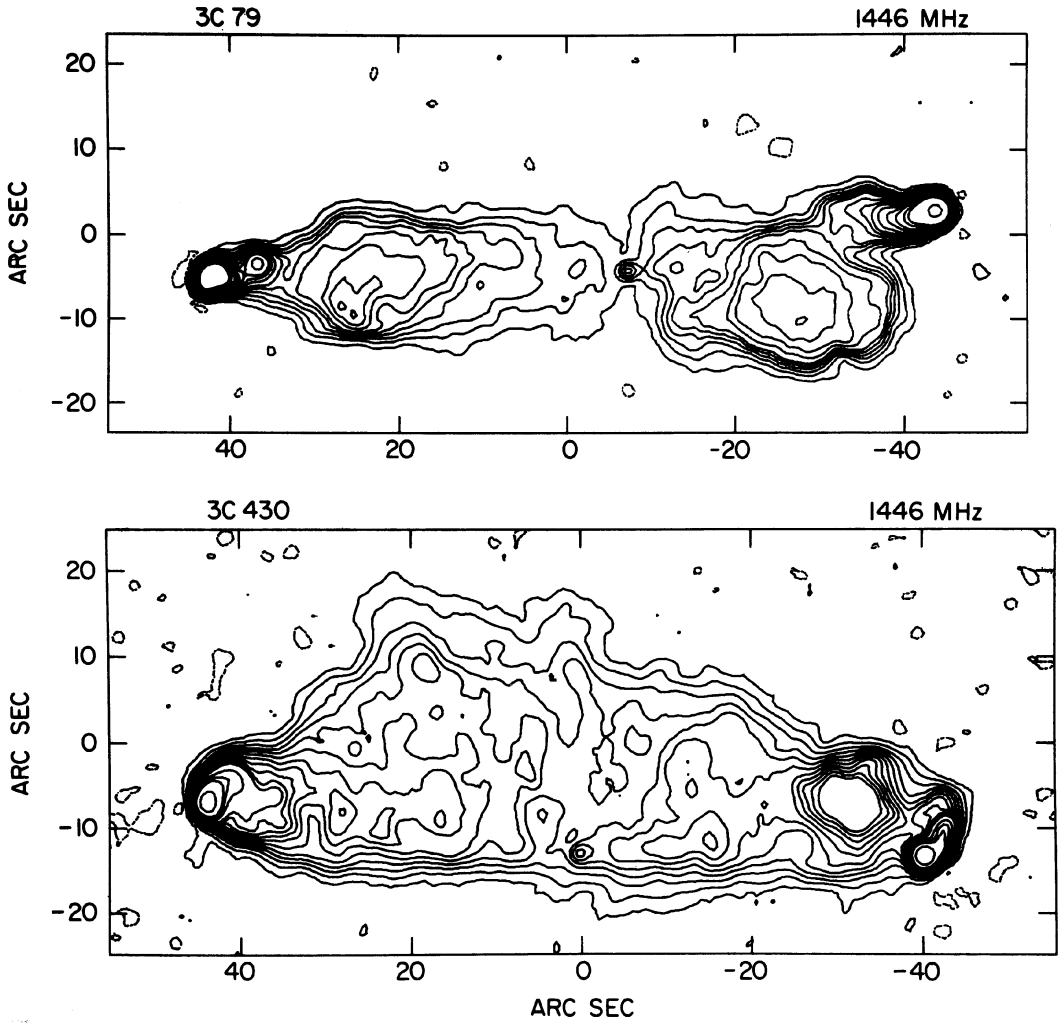

FIG. 1. 1.446-GHz maps of 3C 79 and (b) 3C 430. The images of both sources have been rotated, 3C 79 by − 10° and 3C 430 by 55°. For 3C 79, contours are plotted at − 0.25 (dashed contour), 0.25, 0.75, 1.25, 1.75, 2.25, 3.75, 4.75, 5.75, 7.50, 10.0, 12.5, 17.5, 22.5, and 75 percent of the peak intensity, which is 0.342 Jy/beam. For 3C 430, contours are plotted at − 0.25 (dashed contour), 0.25, 1.0, 2.0, 3.0, 4.0, 5.0, 6.0, 7.0, 8.0, 9.0, 10.0, 15.0, 20.0, 25.0, and 50.0 percent of the peak intensity, which is 0.287 Jy/beam.

TABLE II. Characteristics of central components.

Source	Flux Density (mJy) 1446 MHz	4885 MHz
3C 79	7.8 ± 0.7	10.5 ± 0.5
3C 430	10 ± 2*	11 ± 1
	Position α_{1950}	δ_{1950}
3C 79	$3^h07^m11^s.38$	16°54'37".1
3C 430	$21^h17^m02^s.66$	60°35'27".0

*Greater uncertainty is due to cospatial extended emission.

sesses a shell-like structure in polarized intensity with the inferred magnetic field being tangential to this shell. Substantial depolarization is observed in the lower-left portion of the lobe.

In contrast, the S_f lobe does not display a pronounced shell structure in polarized intensity (although a small increase in fractional polarization does occur near the lobe periphery), and there is little, if any, depolarization.

Panel 2(c) (polarization position angle difference) is striking in that it displays a nearly constant position-angle difference across the face of the source. The only substantial departures from this constant difference are to be found in the aforementioned lower-left parts of the N_p lobe. The minimum Faraday rotation compatible with these observations is a value of − 15.6 rad/m^2, which is in good agreement with the value of − 19 rad/m^2 presented by Simard-Normandin and Kronberg (1980).

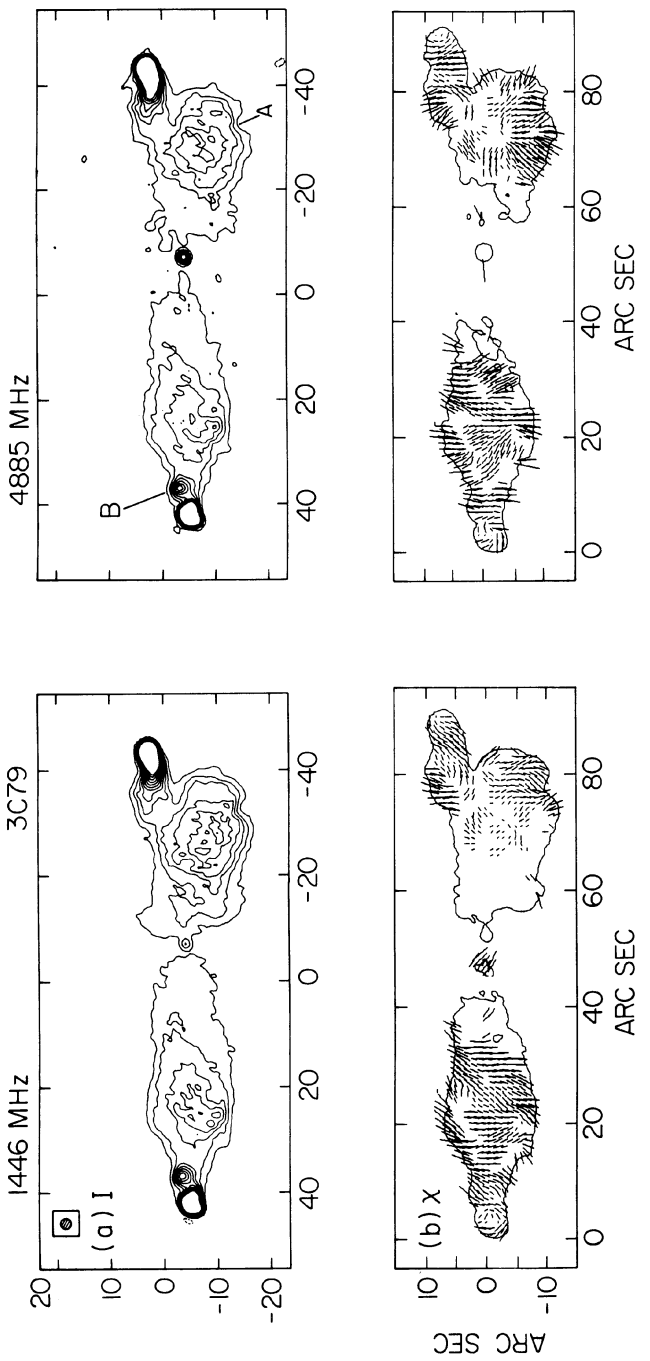

FIG. 2. Dual-frequency maps of 3C 79. Contour plots of total intensity (a) and polarization position angle [$1/2 \tan^{-1}(U/Q)$], (b) are shown in the first two sets of panels. The left-hand set of panels presents 1.446-GHz images, with those at 4.885 GHz being shown in the right-hand set of panels. A polarization position-angle difference map ($\chi_{20} - \chi_6$) is shown in panel (c), and panel (d) presents a coarse-resolution gray-scale map of the spectral-index distribution. The total-intensity images are contoured at the same levels to facilitate comparison. Contours are plotted at intervals of one percent of peak intensity, beginning at -0.5%. The peak intensity is 0.342 Jy/beam at 1.446 GHz, and 0.115 Jy/beam at 4.885 GHz. The lengths of the vectors plotted in panels (b) are proportional to the fractional linear polarization, and regions of low polarized intensity have been blanked. The restoring beam (1".5 FWHM) is indicated in the upper-left corner.

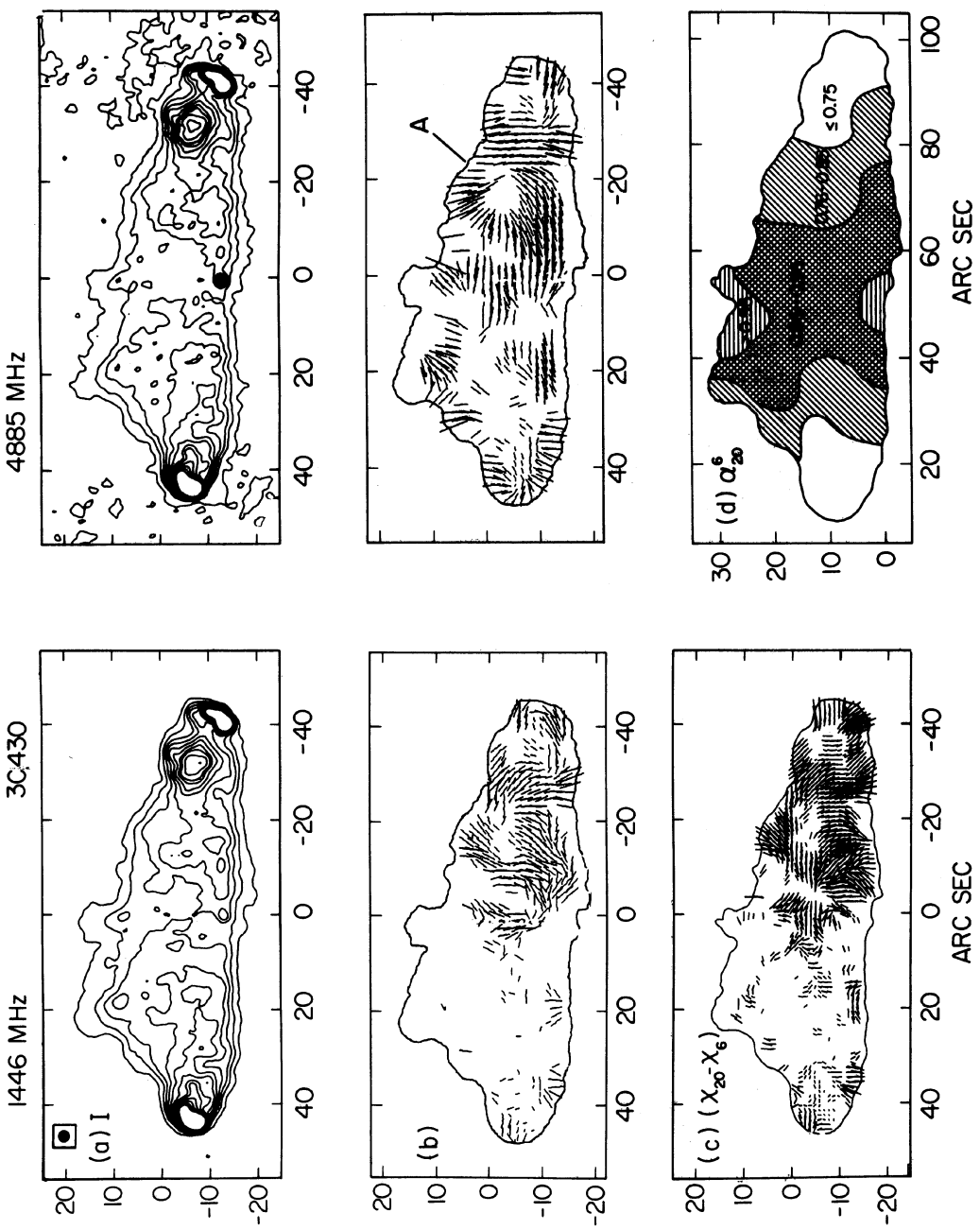

FIG. 3. Dual-frequency maps of 3C 430. The format is the same as Fig. 2. Contours are plotted at intervals of 1.5% of peak intensity, beginning at 0.5%. The peak intensity is 0.287 Jy/beam at 1.446 GHz, and 0.114 Jy/beam at 4.885 GHz. The restoring beam (1".8 FWHM) is indicated in the upper-left corner.

Figure 4 presents map observables along the axis of the S_f lobe. Panel (a) presents the 20-cm intensity, and panels (b) and (c) the fractional linear polarization at 20 and 6 cm. Panel (d) displays the 6–20 cm spectral index, and panel (e) plots the depolarization parameter, defined as the ratio of 6–20 cm fraction linear polarization. The main features to be noted from Fig. 4 are: (1) the fractional linear polarization is relatively low at both frequencies, with no evidence of frequency-dependent depolarization, and (2) the spectral index steepens gradually through the lobe, from a value of about 1.0 near the hot spot, to about 1.2–1.3 in the far extremities of the lobe.

b) 3C 430

In the case of 3C 430, we note a sharp gradient in intensity on the lower side, in contrast to the gradual decrease which occurs in the upper part. This suggests the presence of some agent capable of pressure confinement on the lower side, but which is inhomogeneous on scales of the size of the radio source.

Two features are notable from the polarization observations. First of all, both lobes display a shell-like structure in fractional polarization. Most striking is the ring-like feature indicated as "A" in Fig. 3(b). Furthermore, the entire N_f lobe

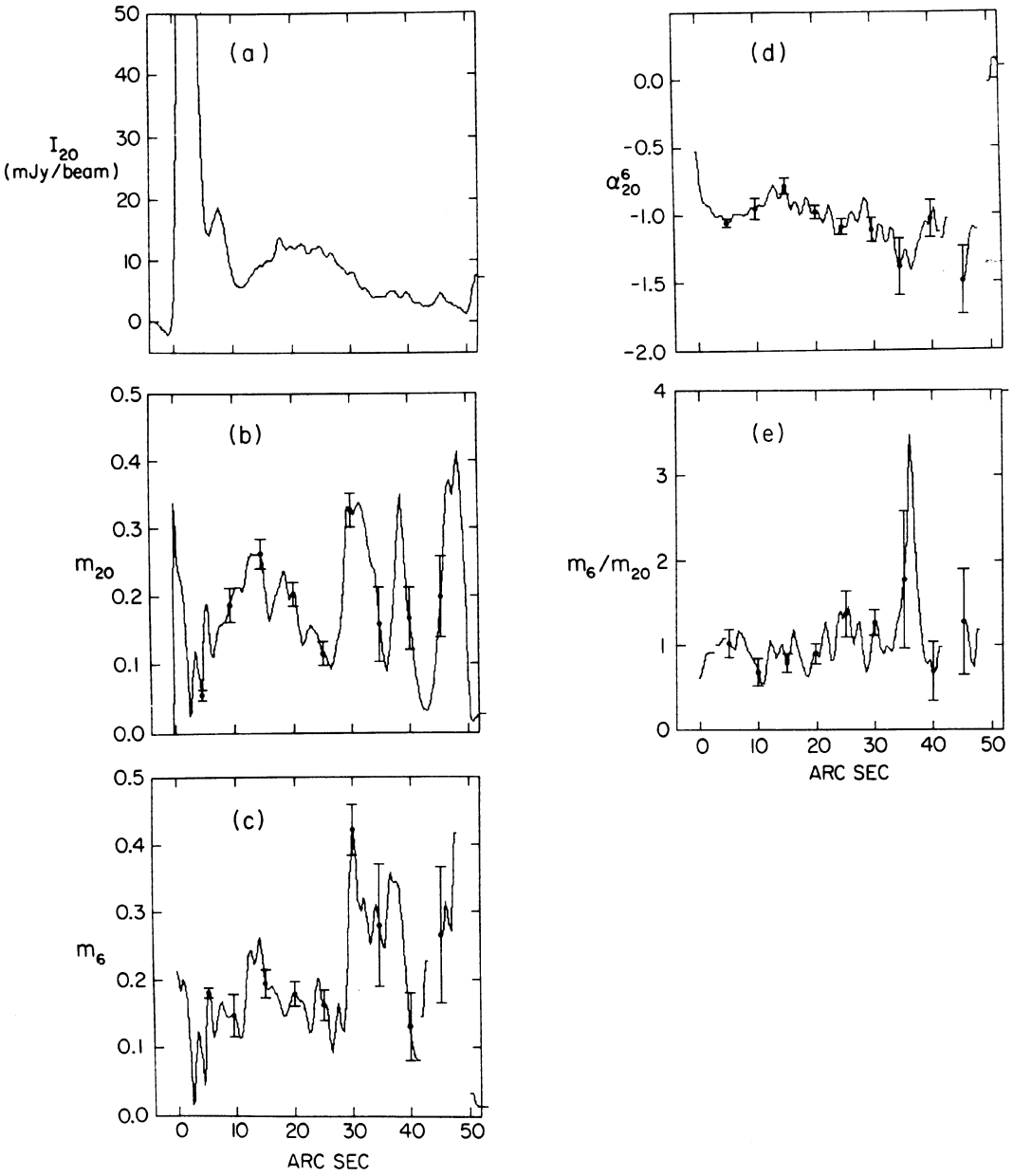

FIG. 4. Map observables along axis of S_f lobe of 3C 79. Display of (a) 20-cm total intensity, (b) fractional linear polarization at 20 cm, (c) fractional linear polarization at 6 cm, (d) depolarization parameter (m_6/m_{20}), and (e) spectral index. Along the axis of this lobe, there is virtually no depolarization, and a gradual steepening of the spectrum.

displays a roughly shell-like structure at 6 cm. This is not the case at 20 cm, possibly due to Faraday depolarization.

Although the two lobes appear very similar in total intensity, the S_p lobe displays little or no depolarization, at least along the source axis, whereas the N_f lobe shows Faraday depolarization.

Before discussing the 5-GHz polarization position angle map and its implication for the magnetic field structure in 3C 430, it is necessary to consider galactic Faraday rotation in the direction of this source. Tabara and Inoue (1980) report an integrated rotation measure of 8.4 ± 4.7 rad/m^2. Our observations tend to support this low value. By far the dominant feature in polarized intensity is the hot spot in the S_p lobe. Our 1.4- and 4.9-GHz observations, together with the 2.7-GHz observations of Burch (1979a,b), yield a rotation measure for the south hot spot which agrees with the Tabara and Inoue value.

The data displayed in Fig. 3(c), the position-angle difference map, are therefore somewhat surprising. Changes in $\Delta\chi$ of at least 90°, corresponding to rotation measure changes $\geqslant 40$ rad/m^2, are observed on angular scales of 10–20 arcsec. In the S_p lobe, where the polarized signal is strongest, these variations are uncorrelated with depolarization, which in any case is quite small. We therefore conclude that these position-angle variations are most likely due to Faraday rotation in a medium external to the source. In view of the galactic coordinates of 3C 430 ($l_{II} = 100°$, $b_{II} = 7°$), it is natural to associate this "screen" with the interstellar medium of our galaxy. However, as noted above, the rotation measure along the line of sight to the hot spot is quite small. Furthermore, the amplitude of the rotation measure fluctuations on these small angular scales is far larger than that expected from turbulence in the interstellar medium of our galaxy (Simonetti *et al.* 1984).

The alternative possibility is that these rotation measure fluctuations arise in material surrounding the radio-emitting lobes, and therefore associated with the 3C 430 galaxy. Evidence of Faraday-rotating clouds surrounding radio-emitting regions has been found in other, albeit smaller, radio galaxies (i.e., Van Breugel *et al.* 1984). With the present data, we can not determine whether these rotation measure fluctuations are galactic or extragalactic in origin.

The existence of these fluctuations affects our ability to determine the structure of the magnetic field in 3C 430. The observed rotation measure changes of 40 rad/m^2 would rotate the 5-GHz position angle 8° from their intrinsic direction. Such a rotation would be discernible, but would not affect our interpretation of the field structure. Naturally, if the rotation measure fluctuations are larger than this, the field structure could not be deduced from our 5-GHz observations.

Assuming that the rotation measure fluctuations are not much larger than the minimum consistent with our observations, we would conclude that the magnetic field of 3C 430 is circumferential in the hot spots and upper side of the source. On the "compressed," lower side of the source, the field is apparently perpendicular to the edge. This differs from what has been seen in our observations of 3C 79, 166, and 411, and may be related to the unusual morphology noted in the total-intensity maps.

The map of spectral index [Fig. 3(d)] shows a symmetry with respect to the two lobes, with spectral index increasing with distance from the hot spot. Throughout most of the source, the change in spectral index is quite small, being of order 0.2.

Many of the observational features referred to above are illustrated in Fig. 5, which displays the variation of map observables along the source axis. Panels (a)–(d) display, respectively, total intensity, fractional linear polarization at 20 and 6 cm, and 6–20 cm spectral index.

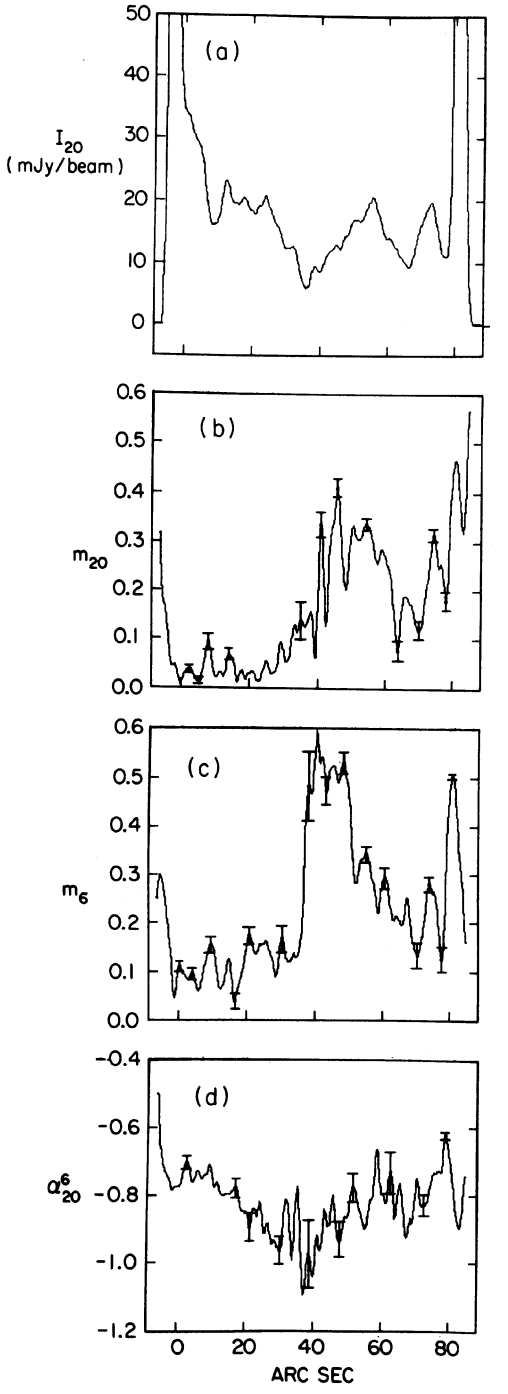

FIG. 5. Map observables along the axis of 3C 430. Displayed are (a) 20-cm total intensity, (b) fractional linear polarization at 20 cm, (c) fractional linear polarization at 6 cm, (d) spectral index. Note the difference in polarization properties of the two lobes.

Figure 5 reveals the pronounced differences in polarization characteristics of the two lobes. In the N_f lobe, the fractional linear polarization is low at both frequencies, but lower at 20 than at 6 cm. This indicates some form of Faraday depolarization is occurring. In the middle of the source, the fractional linear polarization is quite high, again emphasizing the shell structure in linear polarization. The slight difference between the maximum fractional polarization at the two frequencies should be interpreted with caution, as it may be due to geometric depolarization resulting from the Faraday rotating screen. In the S_p lobe, the fractional linear polarization is virtually identical at the two frequencies. Finally, the spectral index shows a smooth variation and is similar in the two lobes.

IV. DISCUSSION

a) Spectral Variations

Both sources possess (relatively modest) spectral index gradients. In 3C 430, we see a smooth steepening of the spectrum with increasing distance from the hot spot. The plot of spectral index versus distance from the hot spot is quite similar in both lobes, indicating similar synchrotron radiation losses. In the N_f lobes of 3C 430, depolarization is observed, allowing one to obtain an estimate of the thermal electron density, if the depolarization is assumed to be internal. We have computed the electron-streaming speed (defined as the rate of separation of the hot spot and lobe material) and Alfvén speed in this lobe, using a method of analysis similar to that described in Spangler and Pogge (1984). A comparison between these speeds is meaningful if electron streaming, rather than hot spot motion, determines the transport of energetic electrons into the lobes. The results are similar to those previously obtained for 3C 166 and 3C 411 (Spangler and Pogge 1984). Under the most favorable circumstances, the Alfvén speed and streaming speed are quite comparable and have a value of about 10^4 km/s, with the streaming speed being higher by about a factor of 2. This would seem to indicate that electron streaming is limited to the Alfvén speed. However, the "most favorable circumstances" may not be realized in practice. They require that: (a) there is a static magnetic field of magnitude equal to the equipartition magnetic field, (b) depolarization is due to this static field, as opposed to magnetic field irregularities, or a screen external to the emitting material, (c) the Faraday depth is the minimum compatible with the observations (i.e., Faraday rotation reduces the degree of polarization at 20, but not at 6 cm), and (d) the source is in the plane of the sky. Violation of these assumptions would have the effect of lowering the Alfvén speed and raising the streaming speed. We feel that some of these assumptions are probably not valid. For example, the static field is probably considerably less than the total, casting doubt on assumption (a). Furthermore, the "minimum Faraday depth" assumption seems questionable in view of our observation (Fig. 5) that the fractional linear polarization at 6 cm increases at a point at which the depolarization decreases. This behavior, which was also observed for 3C 166 and 3C 411, suggests that the Faraday effect is responsible for some of the reduction in 6-cm fractional linear polarization. We therefore consider it likely that the streaming speed significantly exceeds the Alfvén speed. We also note that the similar spectral steepening in the two lobes of 3C 430, which are characterized by quite different polarization properties, suggests that the electron streaming speed may not be determined by the thermal plasma in the lobes.

This type of analysis was not undertaken for 3C 79. The N_p lobe shows a somewhat complicated structure which is not conducive to analysis with simple models. The S_f lobe shows no depolarization, so an Alfvén speed can not be estimated. For this lobe, the spectrum shows behavior similar to that described above for 3C 430, a smooth steepening with increasing distance from the hot spot.

b) Magnetic Field Structures

Our polarimetric observations continue to suggest the ubiquitous appearance of limb-brightened polarized distributions. Such structures are observed in both lobes of 3C 430, and one of the lobes of 3C 79. As has been mentioned in previous publications of ours (Spangler and Bridle 1982; Spangler and Pogge 1984), such structure is consistent with the magnetic fields in the objects being of a highly irregular sort, as proposed by Laing (1981). Laing suggests that magnetic fields in the lobes and other features of extragalactic radio sources are completely random, but possess a minimum variance in the radial direction. This anisotropy is presumed to arise from shearing or compression of the lobe plasma. As discussed by Laing (1981), such a field geometry will produce high degrees of linear polarization near the edges of a lobe, and low-percentage polarization near the center. Although the S_f lobe of 3C 79 does not display a pronounced shell structure, the observations still point to a highly irregular magnetic field. The basis for this statement is given in Fig. 4, which shows that although the fractional polarization is low at both frequencies, the depolarization (again defined as the ratio of 6- to 20-cm fractional polarization) is essentially unity. This indicates that magnetic turbulence, rather than Faraday rotation, is responsible for the reduction in fractional polarization.

An analysis along the lines of Burn (1966) may be used to show that the random component of the magnetic field must be at least twice as large as any static component to account for these polarization observations. We note that the model employed by Burn, that of a static field with superposed, random irregularities, is not compatible with the aforementioned field model of Laing. We employ the Burn formula in the present context merely to show that the random component of the field must be large. We feel that the random field magnitude is *at least* twice that of any static component, since Spangler (1983) has shown that a low, but nonzero, value of the fractional polarization will be observed in the center of a lobe possessing a field of the sort proposed by Laing.

We now wish to consider whether our observations show *any* evidence for large-scale, static magnetic field components, or whether the fields are entirely random, albeit two dimensional, as suggested by Laing. We shall concentrate on our observations of 3C 79; the polarization characteristics of 3C 430 being substantially affected by a foreground Faraday screen.

As noted in Sec. III above, the N_p lobe of 3C 79 displays both depolarization and Faraday rotation (change in $\Delta\chi$). Such characteristics could result from internal Faraday rotation, which would indicate the presence of a large-scale magnetic field. Depolarization can occur in a magnetic field geometry of the type proposed by Laing (provided, of course, that thermal plasma is present), and can be a very strong function of wavelength. However, depolarization should not be accompanied by *systematic* position-angle rotation; the expectation value of the field, and, therefore, the Faraday

depth, is zero. However, if depolarization is due, at least in part, to a static field component, rotation will accompany depolarization.

Measurements of depolarization and position-angle rotation in the N_p lobe of 3C 79 revealed a correlation between depolarization and Faraday rotation which was in reasonable agreement with the relationship expected for a homogeneous, internally depolarized source.

These observations would seem to provide strong evidence for the existence of a large-scale magnetic field which produces internal depolarization. Unfortunately, such a model is not the only one consistent with our observations. Perley, Bridle, and Willis (1984), in their discussion of the radio jet in NGC 6251, point out that earlier, low-resolution observations of this object indicated a correlation between depolarization and position-angle rotation which was interpreted as internal Faraday rotation. Subsequent higher-resolution observations indicated smaller depolarization and revealed rotation measure gradients. Perley, Bridle, and Willis term this effect *false depolarization*; an external Faraday screen produces position-angle changes on a scale comparable to the beam. A resultant drop is seen in the fractional polarization at the lower frequency, even though no internal depolarization is occurring.

We have attempted to determine whether false depolarization is responsible for our observations of 3C 79. Unfortunately, the results are ambiguous. A region is observed in which the positional angle difference changes on the scale of a beam, accompanied by a drop in the fractional polarization. This is consistent with the presence of false depolarization. With the exception of this feature, however, the depolarization does not seem to arise from finite resolution effects, supporting an internal depolarization mechanism.

In summary, a correlation between depolarization and rotation, indicative of internal Faraday depolarization, is observed in the N_p lobe of 3C 79. This correlation persists when measurements affected by finite resolution ("false depolarization") are removed. However, the presence of such finite resolution effects raises questions as to whether rotation measure gradients on still smaller scales might be responsible for all of the observed correlation. It is therefore not clear whether this source possesses internal depolarization, or whether our observations are due to a Faraday rotating screen on the periphery of the source.

V. SUMMARY

The following points summarize our observations of the extended radio galaxies 3C 79 and 3C 430.

(1) The source 3C 430 displays a highly asymmetric shape, being compressed on one side, perhaps by an intergalactic medium. This side is also characterized by a polarization anomaly, with the inferred magnetic field being perpendicular to the edge.

(2) A noncollinear structure is observed in the N_p lobe of 3C 79, in that the lobe and hot spot appear spatially separated.

(3) The spectra in the lobes are seen to continuously steepen with increasing distance from the hot spot. This is consistent with expectation if the electrons are accelerated in the hot spots and subsequently flow out, or are left behind by a moving hot spot. In the N_f lobe of 3C 430, we are able to compare estimates of the particle-streaming speed and Alfvén speed. In the most favorable case, resulting from the simplest analysis, these speeds are comparable, being about 10^4 km/s. This would seem to support the idea that electron streaming is limited to the Alfvén speed. However, it seems that a more realistic analysis would result in a greater discrepancy between the two speeds.

(4) We continue to observe polarized brightness distributions which may be described as limb brightened. This supports the quasi-ordered magnetic field model of Laing (1981). In the case of 3C 79, a correlation between depolarization and Faraday rotation is observed, indicating the existence of internal depolarization and a large-scale, static magnetic field. However, at least part of the effect is due to rotation measure gradients on scales comparable to the beam, an effect termed "false depolarization" by Perley, Bridle, and Willis (1984). At present, it is unclear whether Faraday rotation internal to the source or in an external screen is more important.

This work has been supported by NSF Grant No. AST82-17714.

REFERENCES

Blandford, R. D., and Rees, M. J. (1974). Mon. Not. R. Astron. Soc. **169**, 395.
Burbidge, G. R., and Crowne, A. H. (1979). Astrophys. J. Suppl. **40**, 583.
Burch, S. F. (1977). Mon. Not. R. Astron. Soc. **180**, 623.
Burch, S. F. (1979a). Mon. Not. R. Astron. Soc. **186**, 293.
Burch, S. F. (1979b). Mon. Not. R. Astron. Soc. **186**, 519.
Burn, B. J. (1966). Mon. Not. R. Astron. Soc. **133**, 67.
Laing, R. A. (1981). Mon. Not. R. Astron. Soc. **195**, 261.
Perley, R. A., Bridle, A. H., and Willis, A. G. (1984). Astrophys. J. Suppl. **54**, 291.
Simard-Normandin, M., and Kronberg, P. (1980). Astrophys. J. **242**, 74.
Simonetti, J. H., Cordes, J. M., and Spangler, S. R. (1984). Astrophys. J. (in press).
Spangler, S. R. (1983). Astrophys. J. Lett. **271**, L49.
Spangler, S. R., and Bridle, A. H. (1982). Astron. J. **87**, 1270.
Spangler, S. R., and Pogge, J. J. (1984). Astron. J. **89**, 342.
Tabara, H., and Inoue, M. (1980). Astron. Astrophys. Suppl. **39**, 379.
van Breugel, W., Heckman, T., and Miley, G. (1984). Astrophys. J. **276**, 79.
Winter, A., Wilson, D., Warner, P., Waldram, E., Routledge, D., Nicol, A., Boysen, R., Bly, D., and Baldwin, J. (1980). Mon. Not. R. Astron. Soc. **192**, 931.